



RESEARCH ARTICLE

Neural efficiency and proficiency adaptation of effective connectivity corresponding to early and advanced skill levels in athletes of racket sports

Qing Gao^{1,2,3}  | Ning Luo² | Mengli Sun² | Weiqi Zhou² | Yan Li² |
Minfeng Liang² | Chengbo Yang⁴ | Mu Zhang⁵ | Rong Li³ | Lisha Gong² |
Jiali Yu² | Jinsong Leng² | Huafu Chen^{1,3} 

¹Department of Radiology, First Affiliated Hospital to Army Medical University, Chongqing, People's Republic of China

²School of Mathematical Sciences, University of Electronic Science and Technology of China, Chengdu, People's Republic of China

³The Clinical Hospital of Chengdu Brain Science Institute, MOE Key Laboratory for Neuroinformation, High-Field Magnetic Resonance Brain Imaging Key Laboratory of Sichuan Province, School of Life Science and Technology, University of Electronic Science and Technology of China, Chengdu, People's Republic of China

⁴The Third Department of Physical Education and Training, Chengdu Sport University, Chengdu, People's Republic of China

⁵Information Technology Center, Chengdu Sport University, Chengdu, People's Republic of China

Correspondence

Qing Gao, School of Mathematical Sciences, University of Electronic Science and Technology of China, Chengdu 611731, People's Republic of China.
Email: gaoqing@uestc.edu.cn

Huafu Chen, Department of Radiology, First Affiliated Hospital to Army Medical University, Chongqing 400038, People's Republic of China.
Email: chenhf@uestc.edu.cn

Funding information

National Natural Science Foundation of China, Grant/Award Numbers: 61906034, 62036003, 62173070, 82072006, 82121003, U1808204; the Ministry of Science and Technology of China, Grant/Award Number: 2021ZD0201701; National Administration of Traditional Chinese Medicine, Grant/Award Number: ZYYCXTD-D-202003

Abstract

This study explored how the neural efficiency and proficiency worked in athletes with different skill levels from the perspective of effective connectivity brain network in resting state. The deconvolved conditioned Granger causality (GC) analysis was applied to functional magnetic resonance imaging (fMRI) data of 35 elite athletes (EAs) and 42 student-athletes (SAs) of racket sports as well as 39 normal controls (NCs), to obtain the voxel-wised hemodynamic response function (HRF) parameters representing the functional segregation and effective connectivity representing the functional integration. The results showed decreased time-to-peak of HRF in the visual attention brain regions in the two athlete groups compared with NC and decreased response height in the advanced motor control brain regions in EA comparing to the nonelite groups, suggesting the neural efficiency represented by the regional HRF was different in early and advanced skill levels. GC analysis demonstrated that the GC values within the middle occipital gyrus had a linear trend from negative to positive, suggesting a stepwise “neural proficiency” of the effective connectivity from NC to SA then to EA. The GC values of the inter-lobe circuits in EA had the trend to regress to NC levels, in agreement with the neural efficiency of these circuits in EA. Further feature selection approach suggested the important role of the cerebral-brainstem GC circuit for discriminating EA. Our findings gave new insight into the complementary neural mechanisms in brain functional segregation

This is an open access article under the terms of the [Creative Commons Attribution-NonCommercial-NoDerivs](https://creativecommons.org/licenses/by-nc-nd/4.0/) License, which permits use and distribution in any medium, provided the original work is properly cited, the use is non-commercial and no modifications or adaptations are made.

© 2022 The Authors. *Human Brain Mapping* published by Wiley Periodicals LLC.

and integration, which was associated with early and advanced skill levels in athletes of racket sports.

KEYWORDS

athlete motor training, conditioned Granger causality analysis, hemodynamic response function, neuroplasticity, resting-state functional magnetic resonance imaging

1 | INTRODUCTION

Athletes perform consistently at optimal levels even under challenging conditions (Filho et al., 2021). Key characteristics of optimal performance include a focus on the present, physical, and psychological relaxation (i.e., absence of somatic and cognitive anxiety), high levels of confidence, and effortless “automatic” movement (Filho et al., 2021; Williams & Krane, 2020). The brain supervises the functioning of the entire organic system for adaptive behavior and performance (Bertollo et al., 2020). However, the neural mechanisms underpinning the optimal performance in athletes remain unclear so far. Recent studies suggested that complementary hypotheses neural efficiency and neural proficiency theoretically correlated with optimal performance in experts (Bertollo et al., 2020; Dietrich, 2006; Filho et al., 2021; Holmes & Wright, 2017; Li & Smith, 2021). According to the neural efficiency hypothesis, experts perform better than novices because their brains work smartly by only recruiting the spatiotemporal areas needed to perform the task at hand (Bertollo et al., 2020; Filho et al., 2021; Holmes & Wright, 2017). Neural efficiency can be represented by two different processes. The first indicates that the more the expertise increases, the more the task becomes automated and under less executive control; the second reflects a more efficient processing with a reduction of activity in sensory and motor cortices, made possible by less energy expenditure (Bertollo et al., 2020; Filho et al., 2021).

However, the majority of studies observed the increased activity in athlete in specific brain regions comparing to normal controls (Bertollo et al., 2016; Coffman et al., 2014; Del Percio et al., 2019; Duru & Assem, 2018; Fargier et al., 2017; Filho et al., 2021; Li & Smith, 2021), so the notion that reduced brain activity explains optimal performance experiences has been questioned (Filho et al., 2021). In this regard, Neubauer and Fink (2009) found that the neural efficiency was mostly observed in tasks of easy or moderate complexity (Filho et al., 2021; Neubauer & Fink, 2009). For moderate-to-complex tasks, individuals needed to recruit more cortical resources to perform at an optimal level (Filho et al., 2021; Neubauer & Fink, 2009). The neural proficiency hypothesis was thereby proposed, in which cortical activity is deemed to be related not only to automaticity and economy of effort but also to some degrees of control and exertion needed to effectively execute the task with maximum certainty (Bertollo et al., 2016; Bertollo et al., 2020). Athletes need to engage in both efficient (system-1; fluid and automatic thinking) and effortful (system-2; deliberative thinking) processing to be able to consistently perform at optimal levels (Bertollo et al., 2016; Bertollo et al., 2020; Filho

et al., 2021). In other words, athletes can adeptly use and switch between these two types of processing in order to optimally perform complex tasks under high pressure: (a) purposefully recruit neural networks that allow them to perceive the environment, make decisions, and regulate their thoughts, feelings, and behaviors; and (b) silence the parts of their brains that are not relevant to the task at hand (Filho et al., 2021; Hatfield, 2018; Li & Smith, 2021; Tenenbaum et al., 2013). How the putative neural mechanisms of neural efficiency and neural proficiency work in the athletes' brain to support these neuroplastic adaptation would be of great interests.

The discrepancy of the neuroplasticity representation among the studies aforementioned might be partly attributed to the specific tasks (Filho et al., 2021; Neubauer & Fink, 2009). To avoid the constraints of task-based approaches, the resting-state functional magnetic resonance imaging (fMRI) observes the intrinsically organized spontaneous fluctuations in the blood oxygen level-dependent (BOLD) signal (Gao et al., 2021; Raichle & Snyder, 2007). Therefore, it is an effective approach to study the intrinsic brain plasticity induced by motor learning/training (Gao et al., 2021). The motor training would induce the neuroplasticity in the resting-state brain network has been supported by recent studies (Cantou et al., 2018; Di et al., 2012; Gao et al., 2019). For example, using seed-based functional connectivity (FC), distance runners were found to show enhanced connectivity between the fronto-parietal network and brain regions associated with executive cognitive functions (Raichlen et al., 2016). Badminton players displayed functional alterations in fronto-parietal network (Di et al., 2012). Elite karate players had increased connectivity in the brain regions, which are involved in movement planning and visual perception (Duru & Balcioglu, 2018).

In contrast to the undirected FC, which is defined as temporal correlations between spatially remote neurophysiological events (Friston, 1994), effective connectivity investigates accurately the direct or indirect influence that one neural system exerts over another (Gao et al., 2011, 2016). The Granger causality (GC) analysis has been widely used to explore the effective connectivity among remote brain regions (Gao et al., 2016; Geweke, 1984; Wu et al., 2013). Recently, a blind-deconvolution hemodynamic response function (HRF) retrieval technique was proposed to reconstruct the HRF at each brain voxel. This deconvolution approach took the heterogeneous hemodynamic processes at each brain voxel into account and made it possible to obtain the deconvolved BOLD-level effective connectivity network (Wu et al., 2013). The three parameters of the HRF were applied to characterize the shape of HRF, namely time-to-peak (TTP), response height (RH), and full-width at half-max (FWHM), which were

estimated interpretable in terms of potential measures for latency, response magnitude, and duration of neuronal activity. Physiologically, estimated TTP differences correspond with the behavioral performance or distinguish the responses of one brain region from another, RH differences are associated with either duration increase or activity magnitude increase for brief events, and FWHM differences are attributable to increases in the duration of neuronal activity (Lindquist & Wager, 2007; Wu et al., 2013). Therefore, the three parameters estimated at the voxel level are capable of quantifying regional properties of the brain in resting state (Wu et al., 2013). The adaption of the voxel-specific HRF and effective functional network in resting state of athletes' brain might give us new insight into neural efficiency and neural proficiency corresponding to motor training from the perspective of brain functional segregation and functional integration.

The neuroplastic adaptation induced by motor training would also be associated with different levels of sports experience. There were distinct phases of motor skill training, and the structural and functional adaptation patterns, which were associated with early and advanced stages of motor skill training would be different (Halsband & Lange, 2006). However, most previous studies in sports performance have solely focused on comparing one group of experts with novices, in which potential confounds would arise from differences in participants' experience and extent of training (Chang et al., 2018; Gao et al., 2021; Jancke et al., 2009; Kim et al., 2014). Few studies recruiting athletes with different levels of sports experience demonstrated that a quadratic function instead of a linear relationship could better depict the intergroup differences in structural and functional neuroplasticity (Chang et al., 2018; Gao et al., 2021). Our previous study using dynamic functional connectivity density (dFCD) mapping showed the diversity and specialization of fluctuating dynamic brain adaptation in different training stages, highlighting the effect of motor training stages on brain functional adaptation (Gao et al., 2021).

In the current study, we thereby explored how the neural mechanisms of neural efficiency and neural proficiency worked in the athletes' brain from the perspective of the effective connectivity brain

network in resting state, and if the alterations corresponded to different stages of motor training. We used the blind-deconvolved HRF retrieval technique to reconstruct the HRF at each voxel to detect the voxel-wised variability of HRF in athletes with early and advanced motor training stages. Furthermore, the alterations of the effective connectivity networks at the deconvolved BOLD-level were explored using partially conditioned GC approach (Gao et al., 2011; Wu et al., 2013). We recruited two discriminative athlete groups: the elite-athlete (EA) group (represented the advanced stage of training), and the student-athlete (SA) group (represented the early stage of training). We also recruited the nonathlete health control (NC) group who had little interests or experience in sports. To better understand the contributions of these functional segregation and integration features to the brain function adaption of different skill levels, we further performed the random forest (RF) and recursive feature elimination (RFE) to obtain the optimal features which best differentiated EA, SA, and NC groups (Darst et al., 2018). We hypothesized that the neural mechanisms of neural efficiency and neural proficiency worked differentially in different levels of sports experience, which would be characterized by the voxel-wised HRF representing the local functional segregation and effective connectivity representing the functional integration in resting state.

2 | MATERIALS AND METHODS

2.1 | Participants

We recruited 35 EAs of racket sports (tennis and table tennis) whose training year (i.e., training duration) was longer than 5 years and whose intensity of training (i.e., training intensity) was longer than 28 h per week. All of them won the title of national first-class athletes based on "Athletes Technical Rating Standards" issued by the China General Administration of Sport in 2013 and were recruited from the China University Championships held in Chengdu, China. Forty-two SAs of racket sports whose training year was less than 3 years and training intensity was less than 28 h per week were recruited from

	EA (n = 35)	SA (n = 42)	NC (n = 39)	
	Mean ± SD	Mean ± SD	Mean ± SD	p value
Age (years)	19.43 ± 3.65	20.43 ± 0.59	20.33 ± 1.33	.52 ^a
Gender (female:male)	18:17	12:30	15:24	.12 ^a
Education (years)	13.4 ± 3.3	14.57 ± 0.67	15.05 ± 1.43	.08 ^a
Train time (hours/week)	32.23 ± 4.16	17.17 ± 0.83	-	<.0001 ^{*,b}
Duration (years)	9.94 ± 0.42	1.95 ± 0.08	-	<.0001 ^{*,b}
Mean FD (mm)	0.08 ± 0.03	0.08 ± 0.02	0.08 ± 0.03	.70 ^a

TABLE 1 Demographic and information of subjects

Abbreviations: EA, elite athlete; FD, frame-wise displacement; NC, nonathlete control; SA, student athlete; SD, standard deviation.

^aKruskal-Wallis test.

^bTwo-sample t-test.

*p < .01.

Chengdu Sport University. They were the students from the tennis/table tennis specialty of the physical education major. Thirty-nine NCS with matched age, sex, and education level were also recruited (Table 1). All subjects were right-handed as tested by the Chinese version of Edinburgh-Handedness Questionnaire (coefficients > 50) (Oldfield, 1971) and had no history of neurological or psychiatric diseases or concussions. The current study protocol was approved by the research ethical committee of School of Life Science and Technology, University of Electronic Science, and Technology of China and was carried out under the approved guidelines. The informed written consent has been obtained from all participants.

2.2 | Data acquisition

MRI images were acquired on a 3.0 T GE Signa MR750 system (GE Healthcare, Milwaukee, USA) with an 8-channel-phased array head coil. High-resolution three dimensional (3D) T1-weighted anatomical images were obtained in axial orientation using a 3D spoiled gradient-recalled (SPGR) sequence. The acquisition parameters were as follows: $TR = 5.97$ ms, $TE = 1.96$ ms, field of view (FOV) = 240×240 mm², flip angle = 12° , matrix size = 512×512 , 156 slices, and voxel size = $1 \times 1 \times 1$ mm³. Resting-state fMRI images were acquired using a gradient-recalled echo planar imaging (EPI) sequence. The parameters were: $TR = 2000$ ms, $TE = 30$ ms, FOV = 220×220 mm², flip angle = 90° , matrix size = 64×64 , 43 transverse slices without slice gap, voxel size = $3.75 \times 3.75 \times 3.2$ mm³, and a total of 266 volumes for each subject. During the scan, the subjects were instructed to lie down with their eyes closed, not to think of anything in particular, and not to fall asleep. Padded foams were used to restrict head motion, and earplugs were used to attenuate scanner noise.

2.3 | Data preprocessing

Conventional fMRI data preprocessing was performed using Data Processing Assistant for Resting-State fMRI software (DPARSF, Advanced Edition, V4.3, <http://www.restfmri.net/forum/>). The first 10 volumes of each subject were discarded to ensure steady-state longitudinal magnetization. The remaining 256 resting-state fMRI images were first corrected for the acquisition time delay between different slices and then realigned to the first volume to correct for head motion. We required that the transient movement during the scanning is no more than 2.0 mm of translation and 2.0° of rotation. The images were further spatially normalized into a standard stereotaxic space at $3 \times 3 \times 3$ mm³, using the Montreal Neurological Institute (MNI) template in Statistical Parametric Mapping software (SPM12). The images were not smoothed to avoid introducing artificial local spatial correlations. Images were then linearly detrended and corrected using linear regression to remove the possible spurious variances including 24 head motion parameters, averaged signals from cerebrospinal fluid, and white matter. The residuals of these regressions were temporally band-pass filtered ($0.01 < f < 0.1$ Hz) to

reduce low-frequency drifts and physiological high-frequency respiratory and cardiac noises. Since FC analysis was sensitive to gross head motion effects (Power et al., 2012), the mean frame-wise displacement (FD) was calculated to further determine the comparability of head movement across groups. The largest FD obtained from the subjects was less than 0.2 mm. Note that we did not use the scrubbing method for head motion correction, since the previous study suggested that methods, which are sensitive to temporal ordering in the data cannot use scrubbing (Deshpande et al., 2013). The removal of certain parts of the time series (scrubbing) would create an artificial discontinuity in the data (Deshpande et al., 2013).

2.4 | Blind-deconvolution in resting-state fMRI data

The blind-deconvolution technique for voxel-wise HRF estimation was performed using the NeuroImaging toolbox for Causal Connectome software (NICE, <https://guorongwu.github.io/HRF/>). The three parameters of HRF at each voxel, that is, TTP, RH, and FWHM, were estimated for each subject. To investigate between-group voxel-specific differences in HRF parameters, one-way analysis of variance (ANOVA) was performed, respectively, on each of the three parameters using the SPM12 (<http://www.fil.ion.ucl.ac.uk/spm>). The statistically significant threshold was set for multiple comparisons at the cluster level with $p < .05$ using Gaussian random field (GRF) correction, controlled for age, sex, education, and mean FD. The nonparametric Kruskal–Wallis test would be performed if the normal distribution hypotheses of the variables were violated. The brain regions of interest (ROIs) are then defined as the significant differences in the statistical F map results. Furthermore, the ROIs are applied for subsequent post hoc analysis using the Bonferroni correction ($p < .05$).

2.5 | Voxel-wise conditioned Granger causality analysis

Conditioned GC analysis approach allowed to demonstrate the directed influences from one neural system exerts over another for functional coupling effectively in multivariate data sets. The seed-based conditioned GC analysis was employed to the ROIs at the neural level by deconvolution for each subject. The signed-path coefficients were evaluated in the directed functional networks among the ROIs and the remaining brain voxels using a joint autoregressive model in REST software (V1.8, www.restfmri.net) (Zang et al., 2012). Finally, the directed asymmetric matrix (coefficients matrix) was obtained for each subject.

2.6 | Statistical analysis

To investigate the differences of the effective connectivity networks among the three groups, a one-way ANOVA was performed using

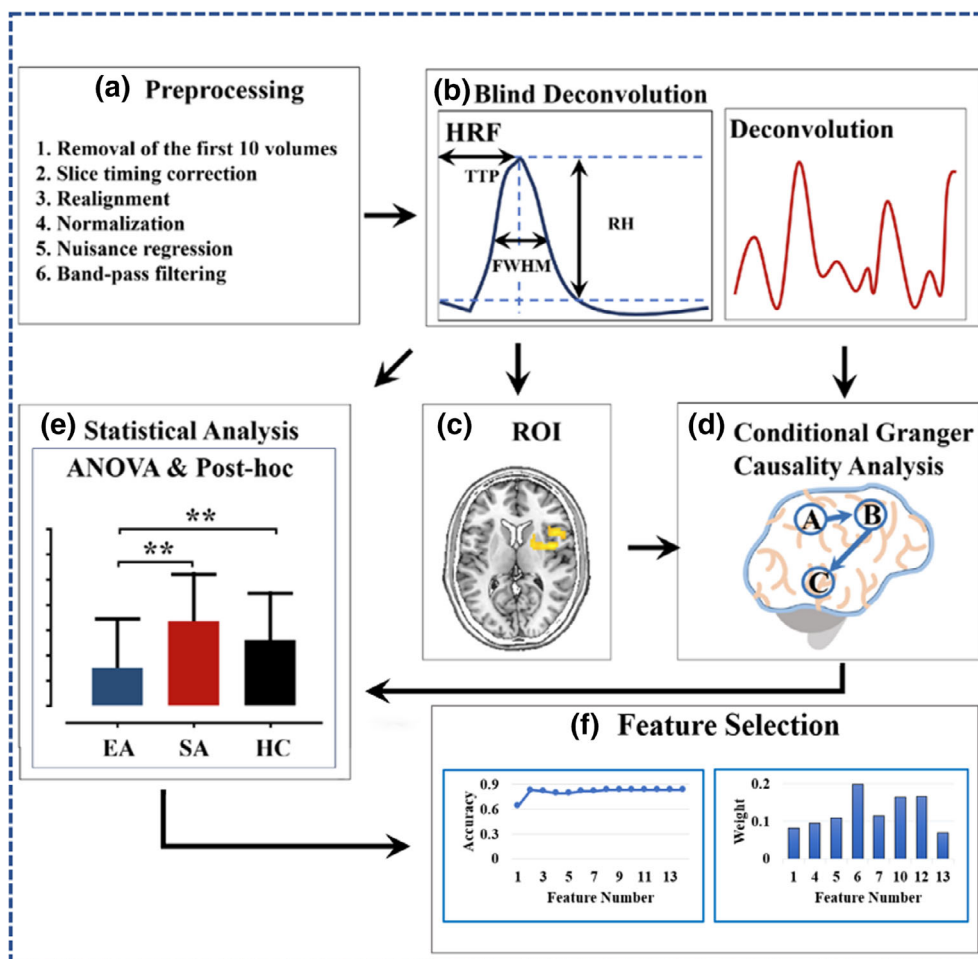


FIGURE 1 The scheme of the data processing. (a) Conventional fMRI data preprocessing using DPARSF. (b) Blind deconvolution to obtain both the voxel-level HRF parameters and the deconvoluted signals. (c) ROI chosen based on ANOVA analysis of the HRF parameters among the three groups. (d) Conditioned GC analysis based on the deconvoluted signals. (e) Statistical analysis. (f) Feature selection. ANOVA, analysis of variance; DPARSF, Data Processing Assistant for Resting-State fMRI; fMRI, functional magnetic resonance imaging; FWHM, full-width at half-max; GC, Granger causality; HRF, hemodynamic response function; RH, response height; ROI, region of interest; TTP, time-to-peak

SPM12. The statistically significant threshold was set at a corrected $p < .05$ by GRF theory to control for multiple comparisons. We regressed out confounding covariates including age, sex, years of education, types of sports, and mean FD. The nonparametric Kruskal-Wallis test would be performed if the normal distribution hypotheses of the variables were violated. Furthermore, the brain regions with significant differences in ANOVA results were selected for subsequent post hoc analysis using the Bonferroni correction ($p < .05$).

2.7 | Feature selection

Using the scikit-learn package, we combined the machine learning algorithm of RF and feature selection algorithm of RFE to obtain the optimal features which best differentiated EA, SA, and NC groups. We evaluated binary classification tasks (EA/SA, SA/NC, and EA/NC) and the multiclass classification task (EA/SA/NC). The RFE is a heuristic feature screening framework which has been widely used to select the most significant features by finding high correlation between specific features and target (labels) (Senan et al., 2021). We used the RFE technique in RF to extract the most significant representative features of a classification (Darst et al., 2018). Basically, (a) we first ran RF to determine initial importance scores, and the classification accuracy of the initial feature subset was

obtained by cross-validation method. (b) Then the feature with the lowest feature importance was removed from the current feature subset, and a new feature was entered into RF to calculate again the importance of each feature in the new feature subset and the classification accuracy of the new feature subset. (c) We repeated step (b) recursively until the feature subset was empty. A total of k subsets with different feature numbers were obtained, the feature subset with the highest classification accuracy was selected as the optimal feature combination. Figure 1a-f shows the scheme of the data processing.

3 | RESULTS

3.1 | Demographics of the participants

The demographic data of the recruited participants are listed in Table 1. The three groups did not differ significantly in age (Kruskal-Wallis test, $p = 0.52$), sex (Kruskal-Wallis test, $p = .12$), education (Kruskal-Wallis test, $p = .08$), or mean FD (Kruskal-Wallis test, $p = 0.70$). The training intensity and training duration were significantly different between the two athlete groups (training intensity, two-sample t -test, $p < .01$; training duration, two-sample t -test, $p < .01$).

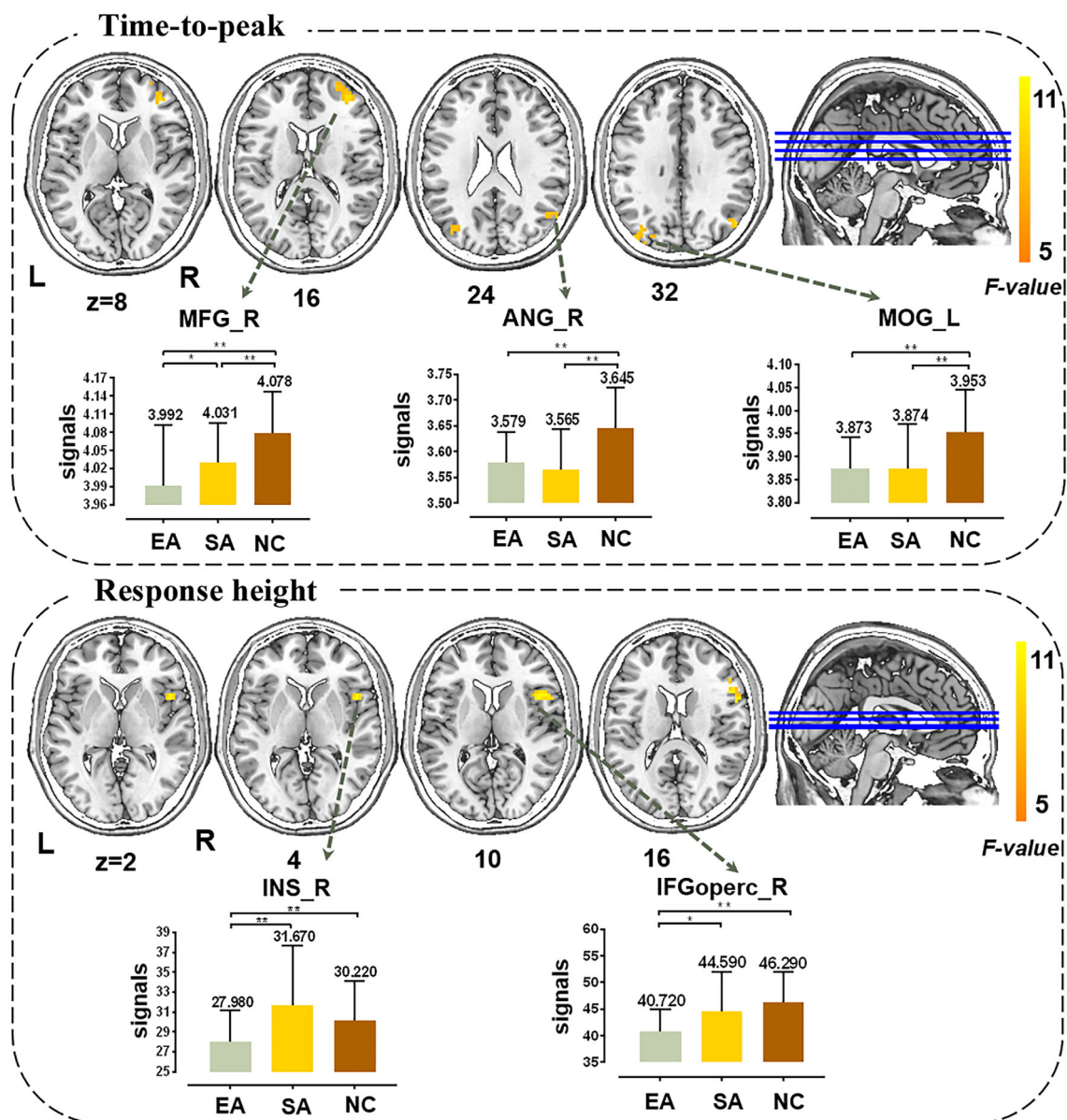


FIGURE 2 The between-group differences of HRF parameters. Upper row: brain regions with significantly different TTP values of HRF among the three groups (one-way ANOVA test, GRF-corrected p value $< .05$). Numbers below each image refer to the z-plane coordinates of the MNI space. Bar graphs indicate the ROI-wise post hoc analysis using two-sample t -tests. The mean TTP values at cluster centroids are also depicted on each bar. Lower row: brain regions with significantly different RH values of HRF among the three groups. Bar graphs indicate the ROI-wise post hoc analysis using two-sample t -tests. The RH values at cluster centroids are also depicted on each bar. ANG, angular gyrus; ANOVA, analysis of variance; EA, elite athlete; GRF, Gaussian random field; HRF, hemodynamic response function; IFGoperc, inferior frontal gyrus opercular part; INS, insula; L, left; MFG, middle frontal gyrus; MNI, Montreal Neurological Institute; MOG, middle occipital gyrus; NC, nonathlete control; R, right; RH, response height; ROI, regions of interest; SA, student athletes; TTP, time-to-peak. * $pp < .05$, uncorrected; ** $p < .05$, Bonferroni corrected

3.2 | HRF variability among the groups

Figure 2 (upper row) demonstrates brain regions with significantly different TTP values of HRF among the three groups (ANOVA, GRF-corrected p -value $< .05$). The statistical analysis showed the significantly different TTP among the three groups in the right middle frontal gyrus (MFG), bilateral middle occipital gyrus (MOG) extending to angular gyrus (ANG). The details of these regions including the MNI

coordinates of peak voxels, statistical F values, and cluster sizes are illustrated in Table 2. Further post hoc t -tests showed that compared with the NC group, the two athlete groups showed significantly decreased HRF TTP in all the ANOVA significant regions.

Figure 2 (lower row) demonstrates the brain regions with significantly different RH values of HRF among the groups (ANOVA, GRF-corrected p value $< .05$). The statistical analysis showed the significantly different RH among the three groups in the right insula (INS)

TABLE 2 Summary of the chosen seeds

Region name	Hem	BA	Coordinates			CS	Peak F-value
			X	Y	Z		
TTP							
Middle frontal gyrus	R	10	39	48	12	38	9.49
Middle occipital gyrus	L	19	-39	-81	30	30	9.34
Angular gyrus	R	39	48	-63	48	20	8.98
RH							
Insula	R		42	0	9	36	9.12
Inferior frontal gyrus, opercular part	R		48	15	6	71	11.24

Abbreviations: ANG, angular gyrus; BA, Brodmann area; CS, cluster size; Hem, hemisphere; IFGoperc, inferior frontal gyrus, opercular part; INS, insula; L, left; MFG, middle frontal gyrus; MOG, middle occipital gyrus; R, right; RH, response height; TTP, time-to-peak.

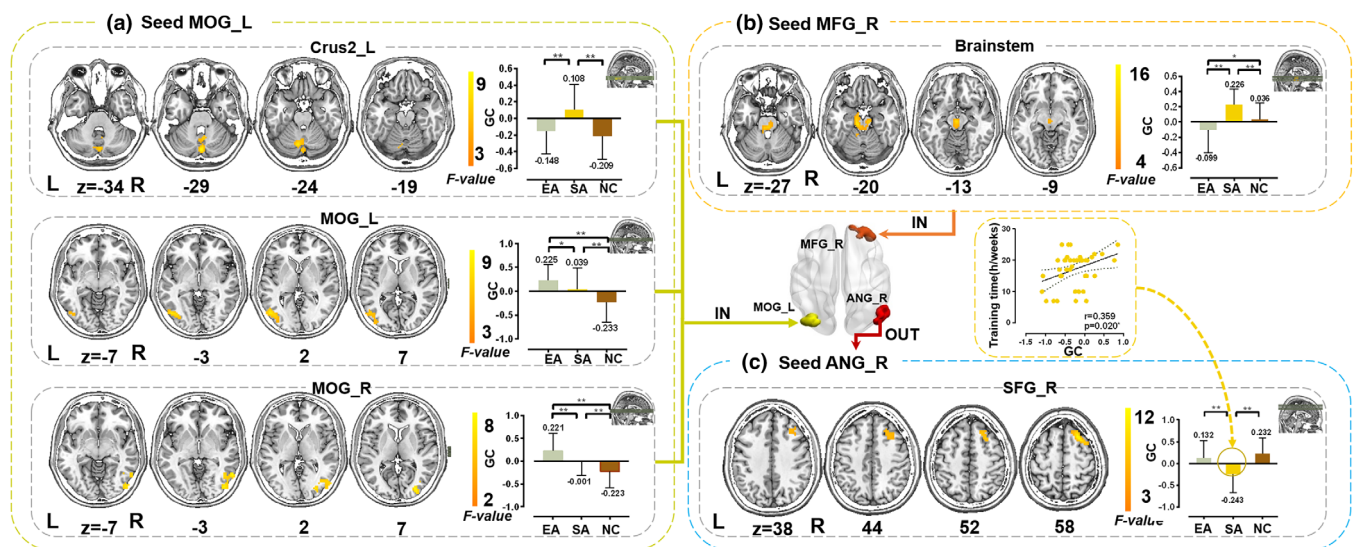


FIGURE 3 Brain regions with significantly different information transfer of TTP-different seeds among the EA, SA, and NC groups. Bar graphs indicating the ROI-wise post hoc analysis using two-sample *t*-tests. The mean signed-path coefficient (GC) values are also depicted on each bar. (a) Seed left MOG; (b) seed right MFG; (c) seed right ANG, where inset depicts that the outflow-GC values from right ANG has significant positive correlation with the training time in SA group. ANG, angular gyrus; Crus2, cerebellum_crus2; EA, elite athlete; GC, Granger causality; MFG, middle frontal gyrus; MOG, middle occipital gyrus; NC, nonathlete health control; ROI, regions of interest; SA, student-athlete; SFG, superior frontal gyrus; TTP, time-to-peak. **p* < .05, uncorrected. ***p* < .05, Bonferroni corrected

and the opercular part of the inferior frontal gyrus (IFGoperc) extending to the inferior frontal gyrus triangular part. The details of these regions including the MNI coordinates of peak voxels, statistical *F* values, and cluster sizes are also illustrated in Table 2. Further post hoc *t*-tests showed that the EA groups showed significantly decreased RH in all the ANOVA significant regions than the SA and NC groups did. Significantly different HRF FWHM among the three groups was not found in the present study.

3.3 | Conditioned Granger causality mapping of significantly different TTP seeds

Significantly different brain regions based on the one-way ANOVA of the HRF parameters were selected as seeds to calculate the

effective connectivity between the seed regions and the remaining brain regions. Figure 3 depicts the brain regions which exhibit significantly different effective connections centered at TTP-different seeds among the three groups (ANOVA, GRF-corrected *p* value < .05). Figure 3a demonstrates the brain regions showing significantly different effective connections to the left MOG seed among the three groups, as well as the post hoc analysis using two-sample *t*-tests. Table 3 summarizes the results in detail. Compared with the SA group, the EA and NC groups exhibited significantly negative GC values from the left cerebellum_crus2 to the left MOG seed. In addition, from NC to SA and then to EA, the GC values from the bilateral MOG/IOG to the MOG seed had a trend from negative to positive.

Figure 3b demonstrates the brain regions, which exhibit significantly different effective connections to the right MFG among the

TABLE 3 Brain regions with significantly different GC values among the three groups

Seed	Region name	Hem	BA	Coordinates	Peak F-value
Right middle frontal gyrus					
Incoming	Brainstem	L	-	(-9, -24, -18)	16.07
Left middle occipital gyrus					
Incoming	Cerebellum_6	L	-	(-9, -69, -24)	10.15
	Middle occipital gyrus	L	37	(-48, -72, 0)	11.66
	Middle occipital gyrus	R	19	(45, -81, 0)	8.5
Right angular gyrus					
Outgoing	Superior frontal gyrus	R	8	(24, 21, 57)	12.87
Right insula					
Outgoing	Brainstem	R	-	(12, -27, -36)	10.92
Incoming	Precuneus	R	7	(6, -63, 39)	7.43
Right inferior frontal gyrus, opercular part					
Outgoing	Superior occipital gyrus	R	7	(21, -69, 36)	8.97
Incoming	Precuneus	R	7	(12, -72, 39)	13.53

Abbreviations: ANG, angular gyrus; BA, Brodmann area; GC, Granger causality; Hem, hemisphere; IFGoperc, inferior frontal gyrus, opercular part; INS, insula; L, left; MFG, middle frontal gyrus; MOG, middle occipital gyrus; R, right; SFG, superior frontal gyrus; SOG, superior occipital gyrus.

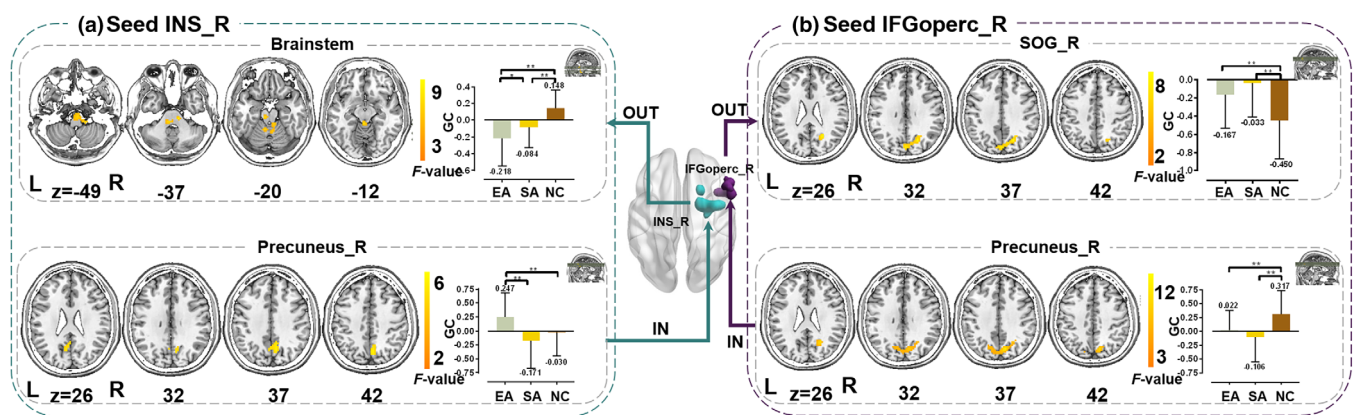


FIGURE 4 Brain regions with significantly different information transfer of RH-different seeds among the EA, SA, and NC groups. Bar graphs indicating the ROI-wise post hoc analysis using two-sample *t*-tests. The mean GC values are also depicted on each bar. (a) Seed right INS. (b) Seed right IFGoperc. EA, elite athlete; GC, Granger causality; IFGoperc, opercular part of the inferior frontal gyrus; INS, insula; NC, nonathlete health control; RH, response height; ROI, regions of interest; SA, student-athlete; SOG, superior occipital gyrus. **p* < .05, uncorrected; ***p* < .05, Bonferroni corrected

three groups. Table 3 summarizes the results in detail. Figure 3b also indicates post hoc analysis using two-sample *t*-tests. Compared with SA, EA and NC exhibited decreased GC values from the brainstem to the right MFG seed. Figure 3c demonstrates the brain regions which exhibit significantly different effective connections from the right ANG among the three groups. The post hoc analysis showed that the EA and NC groups had increased GC values from the right ANG to the right superior frontal gyrus (SFG) than the SA group had. The results further demonstrated that the outflow-GC values from the right ANG to the right SFG had a significant positive correlation with the training time in the SA group ($r = 0.359, p = .020$).

3.4 | Conditioned Granger causality mapping of significant different RH seeds

Figure 4a demonstrates the brain regions which exhibit significantly different effective connections both to and from the right INS among the three groups (ANOVA, GRF-corrected *p* value < .05). The results were summarized in Table 3. Compared with the NC group, the two athlete groups exhibited significantly decreased GC values from the right INS to the brainstem. The excitatory causal inflow from the right precuneus (PCUN) to the right INS was significantly increased in the EA group compared with the other two groups. Figure 4b demonstrates that the right superior occipital gyrus (SOG) shows significantly

TABLE 4 The optimal feature combinations and the importance scores in the classification tasks

Feature	EA versus SA	EA versus NC	SA versus NC	EA versus SA versus NC
TTP: MFG_R	0.082	0.167	0.044	0.143
MOG_L	-	-	0.049	-
ANG_R	-	0.105	0.113	-
RH: INS_R	0.095	-	-	-
IFGoperc_R	0.108	0.144	0.036	0.126
TTP-based GC: brainstem_L to MFG_R	0.199	-	0.091	0.167
cerebellum_L to MOG_L	0.115	-	0.114	-
MOG_L to MOG_L	-	0.126	0.061	-
MOG_R to MOG_L	-	0.155	0.050	-
ANG_R to SFG_R	0.165	-	0.150	0.154
RH-based GC: INS_R to brainstem_R	-	0.186	0.092	0.153
INS_R to PCUN_R	0.167	-	0.029	0.124
IFGoperc_R to SOG_R	0.069	-	0.085	-
IFGoperc_R to PCUN_R	-	0.117	0.087	0.133

Note: Higher values indicate greater contribution of the feature. Different values are highlighted in gradient color of blue.

Abbreviations: ANG, angular gyrus; EA, elite athlete; IFGoperc, inferior frontal gyrus, opercular part; GC, Granger causality; INS, insula; L, left; MFG, middle frontal gyrus; MOG, middle occipital gyrus; NC, nonathlete health control; R, right; RH, response height; SA, student-athlete; TTP, time-to-peak.

different effective connections from the right IFGoperc among the three groups, and that the right PCUN shows significantly different effective connections to the right IFGoperc among the three groups. Table 3 summarizes the results in detail. The post hoc analysis demonstrated that the two athlete groups exhibited significantly increased GC values from the right IFGoperc to the right SOG while significantly decreased GC values from the right PCUN to the right IFGoperc compared with the NC group.

3.5 | Feature selection

The optimal feature combinations in the classification tasks are summarized in Table 4. The best features to differentiate EA and SA were eight features including all RH features and one TTP feature, as well as the GC features (with the classification accuracy of 0.834). The feature with the highest importance score was the GC connectivity from brainstem to right MFG (0.199). Seven features were chosen to best differentiate EA and NC including two TTP features, one RH feature, and four GC features with the classification accuracy of 0.834. The feature with the highest importance score was the GC connectivity from right INS to brainstem (0.186). For discriminating SA and NC, 13 features with all TTP features, one RH feature, and GC features were selected as best features (the classification accuracy: 0.852), in which the GC connectivity from right ANG to right SFG gained the highest score of 0.150. The three groups differentiation relied on seven features including one TTP feature, one RH feature, and five GC features (the classification accuracy: 0.793), in which the GC connectivity from brainstem to right MFG has the highest score of 0.167.

4 | DISCUSSION

To explore how motor training history shapes the brain would be beneficial to sports training, motor learning, and motor rehabilitation in patients with movement disorders (Bertollo et al., 2020; Halsband & Lange, 2006). In addition, its neural mechanism is also the theoretical bases of brain-computer interface. In the present study, we aimed to explore how the neural mechanisms of neural efficiency and neural proficiency worked in the athletes' brain from the perspective of the causal connectivity brain network in resting state, and the possible effect of stages of sports experience on the neuroplasticity. The resting-state research is independent of task and might provide complementary information about functional cerebral reorganization underlying the acquisition, planning, and execution of complex movements and expert actions (Cantou et al., 2018). In addition, we recruited the EA group which represented the advanced stage of training history and the SA group which represented the early stage of training history to expand the knowledge of directed brain network neuroplasticity related to sports experience. Such a design can provide us with the differences of neuroplastic information flow corresponding to different skill levels, and the understanding of the neural mechanism underpinning the optimal performance associated with early and advanced stages of motor learning history (Chang et al., 2018).

4.1 | The HRF adaptation associated with early and advanced stages of training history

The HRF is related to the key physiological factors including cerebral blood flow and the cerebral metabolic rate of oxygen (Handwerker

et al., 2004; Wu et al., 2013; Wu & Marinazzo, 2015). Especially, the TTP has been used to interpret the latency of neural firing (Lindquist & Wager, 2007), and RH has been found to have a striking correlation with cerebral blood flow (Wu & Marinazzo, 2015). According to the “psychomotor efficiency” hypothesis, which posits neural activity is reduced in experts, tennis/table tennis athletes may exhibit faster reaction (i.e., shorter TTP), less brain activation (i.e., lower RH), or shorter brain active time (i.e., FWHM) than nonathletes during the processing of sports related and sports unrelated visuo-spatial tasks (Bertollo et al., 2016; Hatfield, 2018). In the present study, we found that during resting state, the two athlete groups exhibited the decreased TTP values of the HRF in the MFG, MOG, and ANG compared with the NC group, while the EA group exhibited the significantly decreased RH values of the HRF in the INS and the IFG comparing to the SA and NC groups. Our results gave the brain function evidence of the “neural efficiency” hypothesis from the point of view of the HRF and suggested that the neural efficiency of local brain functional segregation in athletes with early stages of motor training history was different from that in athletes with advanced stages of motor training history.

The significantly reduced TTP in the right MFG and bilateral MOG/ANG suggested the shorter latency of neural firing in the athlete groups compared with the NC group. Previous studies have noted that the MFG makes a significant contribution to attention processing, and sustained attention is preferentially controlled by the right MFG during the visual attention task (Song et al., 2019). As a central part of visual perception, the MOG takes part in visual recognition of an object's structure and body-part perception. It is special for spatial than nonspatial visual tasks (Renier et al., 2010). The ANG has connections to the somesthetic and visual cortex and plays a role in permitting cross-modal sensory associations (Smith, 2013). Especially, the ANG is essential for visuospatial awareness. Taken together, our results suggested that appropriate skill levels were likely related to shorter latency of neural firing (represented by reduced TTP) in the brain regions associated with spatial visual attention and visual-motor regulation in the athlete groups. The short latency of neural firing would be fundamental for the fast-pace racket athletes of tennis and table tennis who need to improve visual attention and the ability of visual-motor regulation to accelerate the reaction, movement planning, and execution with high attentional demands (Bertollo et al., 2016; Hatfield, 2018). Another result on the HRF parameters was that compared with the SA and NC groups, the EA group has the significantly reduced RH in the right INS and IFGoperc. Some researchers indicated that the INS was considered to provide motivation for intentional movement when it was involved in processing various sensory signals from self and combining them with emotion and motivation (Tinaz et al., 2018). The IFG plays a critical role in executive control and cognitive functions such as attention control, motor, and behavioral inhibition (Di et al., 2012; Gao et al., 2019; Raichlen et al., 2016; Sie et al., 2019; Wang et al., 2015). Specifically, the right IFGoperc is referred to as action inhibition and execution during the advanced executive control (Hampshire et al., 2010). Our results suggested that the EA group likely had decreased brain metabolism and

altered cerebrovascular physiology in the brain regions associated with motor executive control (Bertollo et al., 2016; Guo et al., 2017; Hatfield, 2018).

Interestingly, the TTP distinguished the athlete groups and the NC group by shorter TTP in the visuospatial attention brain regions in the athlete groups, while the RH differentiated the EA and the nonelite groups by smaller RH in the motor executive control regions in the EA group. Further feature selection approach also showed that the best features to differentiate SA and NC contained all the TTP features while the best features to differentiate EA and SA included all the RH features. It was likely that in the athletes of racket sports, the brain plasticity induced by motor training firstly began in the areas associated with visuospatial attention utilizing a shorter latency of neural firing in the early stage of motor training; then the brain alterations in terms of “psychomotor efficiency” (i.e., lower RH) occurred in the areas related to motor executive control after the athletes underwent the advanced stage of motor training.

4.2 | Effective connectivity adaptation associated with early and advanced stages of training history

To detect the effective connectivity alterations centered at the brain regions with the regional HRF adaptation, the effective connectivity networks between those seeds and the rest of the brain were further computed for each subject. The between-group differences were obtained to explore the neuroplastic adaptation of the brain functional integration by means of effective connectivity. The positive or negative GC values (signed-path coefficients) meant that the past value of a brain region could predict the increased or decreased activity of the present value of another (Zang et al., 2012). The positive causal effect could be interpreted as an excitatory effect and the negative causal effect could be interpreted as an inhibitory effect (Zang et al., 2012). Our results demonstrated that within the primary visual brain regions, the GC values from the bilateral MOG/IOG to the seed left MOG had a trend from negative to positive, from NC to SA and then to EA (Figure 3a). This simple linear trend demonstrated the alterations from inhibitory function to excitatory function, suggesting a stepwise “neural proficiency” from NC to SA then to EA. Similar to the study which revealed an increased gray matter volume of occipital gyrus in the EAs (Chang et al., 2018; Duru & Balcioglu, 2018), our results suggested an increased excitatory causal effect within MOG in the EA group compared with the other two groups. Furthermore, the feature selection approach demonstrated that the best features to differentiate EA/NC and SA/NC both included the GC features from the bilateral MOG/IOG to the seed left MOG, both of which showed the “neural proficiency” effect. The incremental changes of this excitatory function from NC to SA then to EA suggested that the early stage and advanced stage of motor training history played a role in this excitatory function. This might be associated with the consistently increased excitatory regulation in the MOG and enhancement of visual sensory (Engel et al., 2008).

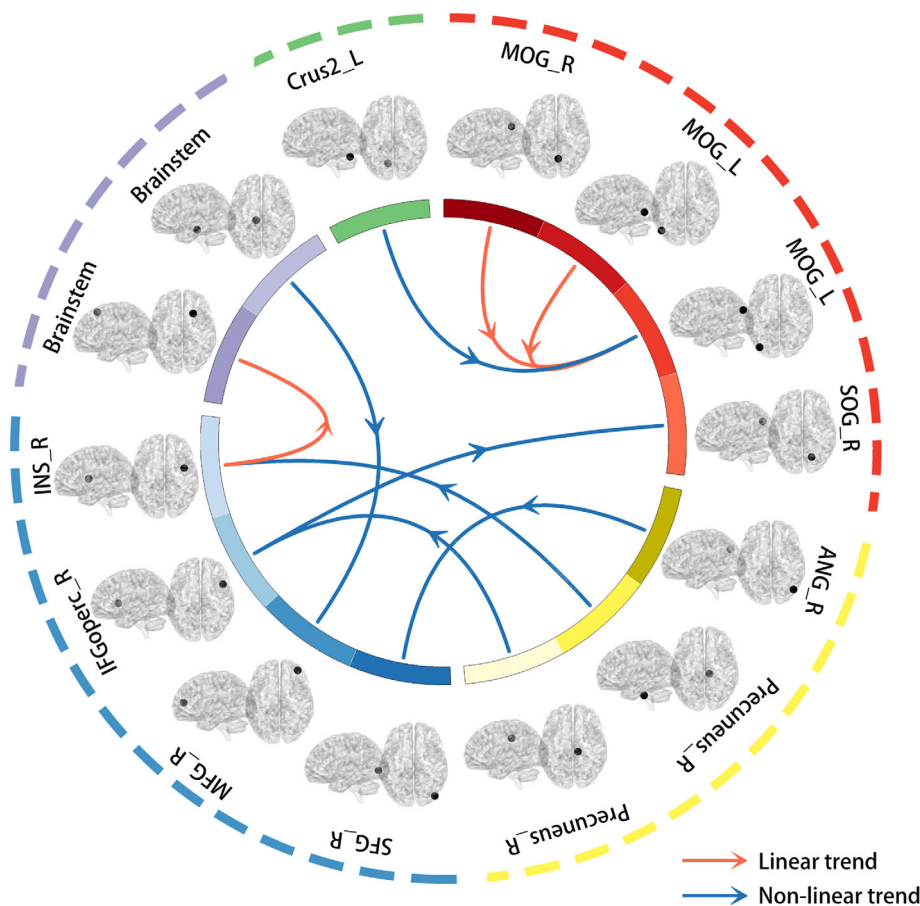


FIGURE 5 The diagram of the between-group significantly different GC connections. The red arrows represent the linear trend of the GC values from the EA group to SA group then to NC group, while the blue arrows represent the nonlinear trend. ANG, angular gyrus; EA, elite athlete; GC, Granger causality; IFGoperc, inferior frontal gyrus opercular part; INS, insula; L, left; MFG, middle frontal gyrus; MOG, middle occipital gyrus; NC, nonathlete controls; R, right; SA, student athlete; SFG, superior frontal gyrus; SOG, superior occipital gyrus

Interestingly, in the fronto-parietal, fronto-occipital, and cerebral-brainstem/cerebellum effective connectivity networks, the GC values in the EA group had the trend to regress to the NC group levels. This nonlinear trend in the networks involving the frontal regions was not the same as the linearly decreasing tendency of the GC values in the MOG. Figure 5 shows the diagram of the between-group significantly different GC connections, in which the red arrows represent the linear trend of the GC values from the EA group to the SA group then to the NC group, while the blue arrows represent the nonlinear trend. This nonlinear trend has been observed in specific brain regions using dFCD variability among the EA, SA, and NC groups in our previous study (Gao et al., 2021). In addition, Chang et al. revealed that a quadratic function could better depict intergroup differences in regional GMV than a linear function among the three groups of skilled baseball batters, intermediate baseball batters, and the NC group (Chang et al., 2018). This nonlinear trend might support the idea of the automation processes of new motor skills in the EA group (Cantou et al., 2018; Zhang et al., 2018). The EA group was able to generate automatic motor behaviors related to the sport after long-term training (Zhang et al., 2018). Therefore, the GC values in these areas related to motor control and visual attention modulation in the EA group had a trend to be at the NC group level. In our study, we further detected a positive correlation between the GC values and the training time in the SA group. The GC values from the right ANG to the right SFG went from negative to positive as training time increased in

the SA group. The SA group has significantly decreased GC values (negative) comparing to the NC group (which had positive GC values); however, the SA group was likely to progressively increase the GC values as training time increased. Further studies on the mechanism of the sharp decrease in the GC values from positive to negative in the SA group comparing to the NC group are expected in the future.

Regarding to the positive and negative GC values, our results also showed the diversity of the fronto-parietal, fronto-occipital, and cerebral-brainstem/cerebellum effective connectivity networks alterations among the three groups. For example, chosen the right IFGoperc as seed, the excitatory causal flow from the right PCUN to the right IFGoperc was significantly decreased, while the inhibitory causal outflow from the right IFGoperc to the right SOG was significantly decreased in the EA and SA groups compared with the NC group (Figure 4b). Some researches on neuroplasticity in athletes showed the resting-state functional alterations in the IFG, especially in the fast-pace racket athletes (Di et al., 2012; Gao et al., 2019; Raichlen et al., 2016; Sie et al., 2019; Wang et al., 2015). Since the PCUN and SOG together are pivotal for conscious visuospatial information processing (Vogt & Laureys, 2005), our results suggested that the training history might relate to the reduced casual influence (regardless of inhibitory or excitatory) between the right IFG and PCUN/SOG associated with motor control and visual attention modulation in the resting state.

4.3 | The cerebral-brainstem GC circuit

The results also showed an increased inhibitory effect from the right INS to the brainstem and from the brainstem to the right MFG in the EA group compared with the NC group; while inconsistent alterations in the SA group compared with the NC group (increased inhibitory effect from the right INS to the brainstem and increased excitatory effect from the brain stem to the right MFG). Specifically, the feature selection results showed that the GC connectivity from brainstem to right MFG gained the highest importance score among the best features in both the binary classification task of EA/SA (0.199) and the multiclass classification task of EA/SA/NC (0.167) (Table 4). In addition, the feature with the highest importance score to discriminate EA and NC was the GC connectivity from right INS to brainstem (0.186). The results suggested the importance of the cerebral-brainstem GC circuit for discriminating the EA subjects. The brainstem plays an important role in the regulation of respiratory and cardiac function, helping to control respiratory rate and heart rate (Benarroch, 2018). Existing literature using fMRI pointed out that hypoxic challenge was associated with activity enhancement in dorsal mid pons within the brainstem (Critchley et al., 2015). In particular, dorsal medullary and pontine activity were inversely correlated with heart rate (Critchley et al., 2015). Some studies demonstrated that activity in the INS and prefrontal cortex showed an inverse relationship with beat-to-beat blood pressure fluctuations (Critchley et al., 2015; Nagai et al., 2010). A study on Macaque has demonstrated that Von Economo neurons, which correlated with consciousness have contributed to interoception by providing inhibitory feedback from INS presumably to earlier (brainstem) levels of interoceptive representation and ultimately supports conscious awareness (Critchley & Seth, 2012; Evrard et al., 2012). Our results demonstrated that the EA group exhibited stronger increased inhibitory regulation from the right INS to the brainstem and from the brainstem to the right MFG compared with the two nonelite groups. The findings extended the previous studies to the effective connectivity network in resting-state, and suggested that the EA group would have an improved capacity of autonomous adjusting the respiratory and heart rate, which might be related to the inhibitory causal flow of the cerebral-brainstem circuit. The inconsistent alterations of the causal flow in the cerebral-brainstem circuit in the SA group might imply the complex process of the brain function alterations in the athletes with early stage of training history, which also needed in-depth research in the future.

4.4 | The consideration of training history stages issue

The post hoc analysis further indicated that the statistical differences of both the HRF shape and the conditioned GC values among the three groups were partly attributed to the differences between the SA and EA groups (i.e., the athletes of the early stage and advanced

stage of motor skill training). Studies in the cognitive psychology of expertise have shown that it is necessary to engage in a sufficient amount of diligent and well-designed deliberate practice to attain expertise (Clementesuares et al., 2016). In various fields, the process of achieving elite performance through arduous self-improvement processes takes an average of 10 years, 4 h/day (Lombardo & Deaner, 2014). Compared with the EA group whose elite performance is relatively stabilized, the SA group is undergoing the process of self-improvement of the motor skill performance. Underlying the functional adaptations in the brains of the two athlete groups, the differential neural mechanisms associated with early and advanced stages of physical exercise or motor training history are thereby of increasing interest (Halsband & Lange, 2006). Studies in large samples reported the decreased FC in the left parietal lobule and frontal-parietal network in athletes who experience a decade of training (Di et al., 2012; Wang et al., 2015). Moreover, many studies showed the increased FC in motor areas as well as in the frontal-parietal network in short-term motor training (Cantou et al., 2018). These results suggested different resting-state connectivity variations depending on the training period (Cantou et al., 2018; Sie et al., 2019). Here, we demonstrated direct evidence of training stage effect on the effective connectivity network of brain in resting state. The motor skill training stages should be considered as a fundamental issue when studying brain adaptation by motor training. The longitudinal study would be designed in the future studies to shed more light on the continuous and incremental neural plasticity by the sports experience.

4.5 | Limitations

Several limitations of the present study are worth mentioning. First, the BOLD signal does not correlate perfectly with action potentials, but rather measures a mix of continuous membrane potentials and action potentials (Logothetis & Wandell, 2004). Therefore, HRF is a complex, nonlinear function of the results of neuronal and vascular changes (Lindquist & Wager, 2007; Logothetis & Wandell, 2004). The parameters of HRF were affected by many physiological sources such as circulatory system in addition to neuronal changes (Lindquist & Wager, 2007; Logothetis & Wandell, 2004; Wager et al., 2005). This is the methodological drawback in fMRI studies. However, finding significant differences of the parameters would still constitute the scientific evidence that may distinguish the responses of one brain region from another (Lindquist & Wager, 2007). Second, the athlete groups showed significantly shorter TTP in the brain regions associated with spatial visual attention and visual-motor regulation compared with the NC group. Further research on the correlation between attentional behavioral performance and the TTP parameters would be helpful to better understand the relationship between the latency of neural firing and the improved ability of the visual attention and visual-motor regulation in the athlete groups. However, we were not able to collect the attention behavior data in the participants. Future study would take this into consideration.

5 | CONCLUSION

Using the resting-state functional imaging techniques, blind deconvolution approach, conditioned GC analysis, and feature selection method, the present study first explored the altered HRF shape among the EA, SA, and NC groups to detect the neuroplastic adaptation of local brain functional segregation. The results gave the brain functional evidence of the “neural efficiency” hypothesis from the point of view of HRF in resting state and suggested that the HRF parameters specified to the early and advanced training history stages, respectively. Further conditioned GC analysis showed the neuroplastic alteration of brain functional integration by means of effective connectivity network in resting state. Specifically, the results demonstrated an increased excitatory regulation within the primary visual sensory regions in athletes, suggesting a stepwise “neural proficiency” from the NC to SA then to EA group. The results also showed the diversity of the fronto-parietal, fronto-occipital, and cerebral-brainstem/cerebellum effective connectivity alterations among the three groups, where the GC values in the EA group had the trend to regress to the NC levels. This was in agreement with the neural efficiency hypothesis which supported the idea of an automation process of new motor skills in these circuits in EA; therefore, the GC values in these areas related to motor control and visual attention modulation had a trend to be at the NC group level. Not like the consistent “neural efficiency” in local HRF in the athlete groups, the GC results suggested a more complex pattern, exhibiting the causal connectivity representation of the complementary neural mechanisms of neural efficiency and neural proficiency. Moreover, the feature selection results demonstrated the role of the inhibitory cerebral-brainstem GC circuit for discriminating the EA subjects, implying the importance of improved capacity of autoregulating the respiratory and heart rate in athletes with advanced skill levels. The neural mechanisms of functional adaptations in the athletes' brain with early and advanced stages of motor training might have potential applications in designing optimal sports coaching methods, in overcoming learning disabilities, and in neurological rehabilitation.

ACKNOWLEDGMENTS

The authors would like to thank Lintao Cheng, Yu Sui, and Xiaolong Su for their assistance in MRI data acquisition, and Guorong Wu for helpful discussion. The work is supported by the Ministry of Science and Technology of China (2021ZD0201701), the National Natural Science Foundation of China (62173070, 82121003, 62036003, U1808204, 82072006, and 61906034), and the Innovation Team and Talents Cultivation Program of National Administration of Traditional Chinese Medicine (ZYYCXTD-D-202003).

DATA AVAILABILITY STATEMENT

The data and code are available via a request to the corresponding author. The data are for research use only.

ORCID

Qing Gao  <https://orcid.org/0000-0001-8504-6128>

Huafu Chen  <https://orcid.org/0000-0002-4062-4753>

REFERENCES

- Benarroch, E. E. (2018). Brainstem integration of arousal, sleep, cardiovascular, and respiratory control. *Neurology*, 91(21), 958–966. <https://doi.org/10.1212/WNL.0000000000006537>
- Bertollo, M., di Fronso, S., Filho, E., Conforto, S., Schmid, M., Bortoli, L., Comani, S., & Robazza, C. (2016). Proficient brain for optimal performance: The MAP model perspective. *PeerJ*, 4, e2082. <https://doi.org/10.7717/peerj.2082>
- Bertollo, M., Doppelmayr, M., & Robazza, C. (2020). Using brain technologies in practice. In G. Tenenbaum & R. C. Eklund (Eds.), *Handbook of sport psychology*. John Wiley & Sons.
- Cantou, P., Platel, H., Desgranges, B., & Groussard, M. (2018). How motor, cognitive and musical expertise shapes the brain: Focus on fMRI and EEG resting-state functional connectivity. *Journal of Chemical Neuroanatomy*, 89, 60–68. <https://doi.org/10.1016/j.jchemneu.2017.08.003>
- Chang, C. Y., Chen, Y. H., & Yen, N. S. (2018). Nonlinear neuroplasticity corresponding to sports experience: A voxel-based morphometry and resting-state functional connectivity study. *Human Brain Mapping*, 39(11), 4393–4403. <https://doi.org/10.1002/hbm.24280>
- Clementesuarez, V. J., Dalamitros, A. A., & Nikolaidis, P. T. (2016). The effect of a short-term training period on physiological parameters and running performance: Intensity distribution versus constant-intensity exercise. *Journal of Sports Medicine and Physical Fitness*, 58, 1–7. <https://doi.org/10.23736/S0022-4707.16.06756-6>
- Coffman, B. A., Clark, V. P., & Parasuraman, R. (2014). Battery powered thought: Enhancement of attention, learning, and memory in healthy adults using transcranial direct current stimulation. *NeuroImage*, 85(Pt 3), 895–908. <https://doi.org/10.1016/j.neuroimage.2013.07.083>
- Critchley, H., & Seth, A. (2012). Will studies of macaque insula reveal the neural mechanisms of self-awareness? *Neuron*, 74(3), 423–426. <https://doi.org/10.1016/j.neuron.2012.04.012>
- Critchley, H. D., Nicotra, A., Chiesa, P. A., Nagai, Y., Gray, M. A., Minati, L., & Bernardi, L. (2015). Slow breathing and hypoxic challenge: Cardiorespiratory consequences and their central neural substrates. *PLoS One*, 10(5), e0127082. <https://doi.org/10.1371/journal.pone.0127082>
- Darst, B. F., Malecki, K. C., & Engelman, C. D. (2018). Using recursive feature elimination in random forest to account for correlated variables in high dimensional data. *BMC Genetics*, 19(Suppl 1), 65. <https://doi.org/10.1186/s12863-018-0633-8>
- Del Percio, C., Franzetti, M., De Matti, A. J., Noce, G., Lizio, R., Lopez, S., Soricelli, A., Ferri, R., Pascarelli, M. T., Rizzo, M., Triggiani, A. I., Stocchi, F., Limatola, C., & Babiloni, C. (2019). Football players do not show “neural efficiency” in cortical activity related to visuospatial information processing during football scenes: An EEG mapping study. *Frontiers in Psychology*, 10, 890. <https://doi.org/10.3389/fpsyg.2019.00890>
- Deshpande, G., Libero, L. E., Sreenivasan, K. R., Deshpande, H. D., & Kana, R. K. (2013). Identification of neural connectivity signatures of autism using machine learning. *Frontiers in Human Neuroscience*, 7, 670. <https://doi.org/10.3389/fnhum.2013.00670>
- Di, X., Zhu, S., Jin, H., Wang, P., Ye, Z., Zhou, K., Zhuo, Y., & Rao, H. (2012). Altered resting brain function and structure in professional badminton players. *Brain Connectivity*, 2(4), 225–233. <https://doi.org/10.1089/brain.2011.0050>
- Dietrich, A. (2006). Transient hypofrontality as a mechanism for the psychological effects of exercise. *Psychiatry Research*, 145(1), 79–83. <https://doi.org/10.1016/j.psychres.2005.07.033>
- Duru, A. D., & Assem, M. (2018). Investigating neural efficiency of elite karate athletes during a mental arithmetic task using EEG. *Cognitive Neurodynamics*, 12(1), 95–102. <https://doi.org/10.1007/s11571-017-9464-y>

- Duru, A. D., & Balcioglu, T. H. (2018). Functional and structural plasticity of brain in elite karate athletes. *Journal of Healthcare Engineering*, 2018, 8310975. <https://doi.org/10.1155/2018/8310975>
- Engel, A., Burke, M., Fiehler, K., Bien, S., & Rösler, F. (2008). Motor learning affects visual movement perception. *European Journal of Neuroscience*, 27(9), 2294–2302. <https://doi.org/10.1111/j.1460-9568.2008.06200.x>
- Evrard, H. C., Forro, T., & Logothetis, N. K. (2012). Von Economo neurons in the anterior insula of the macaque monkey. *Neuron*, 74(3), 482–489. <https://doi.org/10.1016/j.neuron.2012.03.003>
- Fargier, P., Collet, C., Moran, A., & Massarelli, R. (2017). Inter-disciplinary in sport sciences: The neuroscience example. *European Journal of Sport Science*, 17(1), 42–50. <https://doi.org/10.1080/17461391.2016.1207710>
- Filho, E., Dobersek, U., & Husselman, T. A. (2021). The role of neural efficiency, transient hypofrontality and neural proficiency in optimal performance in self-paced sports: A meta-analytic review. *Experimental Brain Research*, 239(5), 1381–1393. <https://doi.org/10.1007/s00221-021-06078-9>
- Friston, K. J. (1994). Functional and effective connectivity in neuroimaging: A synthesis. *Human Brain Mapping*, 2(1–2), 56–78. <https://doi.org/10.1002/hbm.460020107>
- Gao, Q., Duan, X., & Chen, H. (2011). Evaluation of effective connectivity of motor areas during motor imagery and execution using conditional Granger causality. *NeuroImage*, 54(2), 1280–1288. <https://doi.org/10.1016/j.neuroimage.2010.08.071>
- Gao, Q., Huang, Y., Xiang, Y., Yang, C., Zhang, M., Guo, J., Wang, H., Yu, J., Cui, Q., & Chen, H. (2021). Altered dynamics of functional connectivity density associated with early and advanced stages of motor training in tennis and table tennis athletes. *Brain Imaging and Behavior*, 15(3), 1323–1334. <https://doi.org/10.1007/s11682-020-00331-5>
- Gao, Q., Yu, Y., Su, X., Tao, Z., Zhang, M., Wang, Y., Leng, J., Sepulcre, J., & Chen, H. (2019). Adaptation of brain functional stream architecture in athletes with fast demands of sensorimotor integration. *Human Brain Mapping*, 40(2), 420–431. <https://doi.org/10.1002/hbm.24382>
- Gao, Q., Zou, K., He, Z., Sun, X., & Chen, H. (2016). Causal connectivity alterations of cortical-subcortical circuit anchored on reduced hemodynamic response brain regions in first-episode drug-naive major depressive disorder. *Scientific Reports*, 6(2045–2322), 21861. <https://doi.org/10.1038/srep21861>
- Geweke, J. F. (1984). Measures of conditional linear dependence and feedback between time series. *Journal of the American Statistical Association*, 79(388), 907–915. <https://doi.org/10.1080/01621459.1984.10477110>
- Guo, Z., Li, A., & Yu, L. (2017). "Neural efficiency" of athletes' brain during visuo-spatial task: An fMRI study on table tennis players. *Frontiers in Behavioral Neuroscience*, 11, 72. <https://doi.org/10.3389/fnbeh.2017.00072>
- Halsband, U., & Lange, R. K. (2006). Motor learning in man: A review of functional and clinical studies. *Journal of Physiology-Paris*, 99(4), 414–424. <https://doi.org/10.1016/j.jphysparis.2006.03.007>
- Hampshire, A., Chamberlain, S. R., Monti, M. M., Duncan, J., & Owen, A. M. (2010). The role of the right inferior frontal gyrus: Inhibition and attentional control. *NeuroImage*, 50(3), 1313–1319. <https://doi.org/10.1016/j.neuroimage.2009.12.109>
- Handwerker, D. A., Ollinger, J. M., & D'Esposito, M. (2004). Variation of BOLD hemodynamic responses across subjects and brain regions and their effects on statistical analyses. *NeuroImage*, 21(4), 1639–1651. <https://doi.org/10.1016/j.neuroimage.2003.11.029>
- Hatfield, B. D. (2018). Brain dynamics and motor behavior: A case for efficiency and refinement for superior performance. *Kinesiology Review*, 7(1), 42–50.
- Holmes, P. S., & Wright, D. J. (2017). Motor cognition and neuroscience in sport psychology. *Current Opinion in Psychology*, 16, 43–47. <https://doi.org/10.1016/j.copsyc.2017.03.009>
- Jancke, L., Koeneke, S., Hoppe, A., Rominger, C., & Hanggi, J. (2009). The architecture of the golfer's brain. *PLoS One*, 4(3), e4785. <https://doi.org/10.1371/journal.pone.0004785>
- Kim, W., Chang, Y., Kim, J., Seo, J., Ryu, K., Lee, E., Woo, M., & Janelle, C. M. (2014). An fMRI study of differences in brain activity among elite, expert, and novice archers at the moment of optimal aiming. *Cognitive and Behavioral Neurology*, 27(4), 173–182. <https://doi.org/10.1097/WNN.0000000000000042>
- Li, L., & Smith, D. M. (2021). Neural efficiency in athletes: A systematic review. *Frontiers in Behavioral Neuroscience*, 15, 698555. <https://doi.org/10.3389/fnbeh.2021.698555>
- Lindquist, M. A., & Wager, T. D. (2007). Validity and power in hemodynamic response modeling: A comparison study and a new approach. *Human Brain Mapping*, 28(8), 764–784. <https://doi.org/10.1002/hbm.20310>
- Logothetis, N. K., & Wandell, B. A. (2004). Interpreting the BOLD signal. *Annual Review of Physiology*, 66, 735–769. <https://doi.org/10.1146/annurev.physiol.66.082602.092845>
- Lombardo, M. P., & Deane, R. O. (2014). You can't teach speed: Sprinters falsify the deliberate practice model of expertise. *PeerJ*, 2, e445. <https://doi.org/10.7717/peerj.445>
- Nagai, M., Hoshida, S., & Kario, K. (2010). The insular cortex and cardiovascular system: A new insight into the brain-heart axis. *Journal of the American Society of Hypertension*, 4(4), 174–182. <https://doi.org/10.1016/j.jash.2010.05.001>
- Neubauer, A. C., & Fink, A. (2009). Intelligence and neural efficiency. *Neuroscience and Biobehavioral Reviews*, 33(7), 1004–1023. <https://doi.org/10.1016/j.neubiorev.2009.04.001>
- Oldfield, R. C. (1971). The assessment and analysis of handedness: The Edinburgh inventory. *Neuropsychologia*, 9(1), 97–113. [https://doi.org/10.1016/0028-3932\(71\)90067-4](https://doi.org/10.1016/0028-3932(71)90067-4)
- Power, J. D., Barnes, K. A., Snyder, A. Z., Schlaggar, B. L., & Petersen, S. E. (2012). Spurious but systematic correlations in functional connectivity MRI networks arise from subject motion. *NeuroImage*, 59(3), 2142–2154. <https://doi.org/10.1016/j.neuroimage.2011.10.018>
- Raichle, M. E., & Snyder, A. Z. (2007). A default mode of brain function: A brief history of an evolving idea. *NeuroImage*, 37(4), 1083–1090; discussion 1097–1089. <https://doi.org/10.1016/j.neuroimage.2007.02.041>
- Raichlen, D. A., Bharadwaj, P. K., Fitzhugh, M. C., Haws, K. A., Torre, G. A., Trouard, T. P., & Alexander, G. E. (2016). Differences in resting state functional connectivity between young adult endurance athletes and healthy controls. *Frontiers in Human Neuroscience*, 10, 610. <https://doi.org/10.3389/fnhum.2016.00610>
- Renier, L. A., Anurova, I., De Volder, A. G., Carlson, S., VanMeter, J., & Rauschecker, J. P. (2010). Preserved functional specialization for spatial processing in the middle occipital gyrus of the early blind. *Neuron*, 68(1), 138–148. <https://doi.org/10.1016/j.neuron.2010.09.021>
- Senan, E. M., Al-Adhaileh, M. H., Alsaade, F. W., Aldhyani, T. H. H., Alqarni, A. A., Alsharif, N., Uddin, I., Alahmadi, A. H., Jadhav, M. E., & Alzahrani, M. Y. (2021). Diagnosis of chronic kidney disease using effective classification algorithms and recursive feature elimination techniques. *Journal of Healthcare Engineering*, 2021, 1004767. <https://doi.org/10.1155/2021/1004767>
- Sie, J. H., Chen, Y. H., Chang, C. Y., Yen, N. S., Chu, W. C., & Shiau, Y. H. (2019). Altered central autonomic network in baseball players: A resting-state fMRI study. *Scientific Reports*, 9(1), 110. <https://doi.org/10.1038/s41598-018-36329-9>
- Smith, G. E. (2013). The angular gyrus model of consciousness. *PeerJ Pre-Prints*, 1, e22v22. <https://doi.org/10.7287/peerj.preprints.22v2>
- Song, P., Lin, H., Liu, C., Jiang, Y., Lin, Y., Xue, Q., Xu, P., & Wang, Y. (2019). Transcranial magnetic stimulation to the middle frontal gyrus during attention modes induced dynamic module reconfiguration in brain networks. *Frontiers in Neuroinformatics*, 13, 22.

- Tenenbaum, G., Basevitch, I., Gershgoren, L., & Filho, E. (2013). Emotions-decision-making in sport: Theoretical conceptualization and experimental evidence. *International Journal of Sport and Exercise Psychology*, 11(2), 151–168. <https://doi.org/10.1080/1612197X.2013.773687>
- Tinaz, S., Para, K., Vives-Rodriguez, A., Martinez-Kaigi, V., Nalamada, K., Sezgin, M., Scheinost, D., Hampson, M., Louis, E. D., & Constable, R. T. (2018). Insula as the interface between body awareness and movement: A neurofeedback-guided kinesthetic motor imagery study in Parkinson's disease. *Frontiers in Human Neuroscience*, 12, 496.
- Vogt, B. A., & Laureys, S. (2005). Posterior cingulate, precuneal and retrosplenial cortices: Cytology and components of the neural network correlates of consciousness. In S. Laureys (Ed.), *Progress in brain research* (Vol. 150, pp. 205–217). Elsevier.
- Wager, T. D., Vazquez, A., Hernandez, L., & Noll, D. C. (2005). Accounting for nonlinear BOLD effects in fMRI: Parameter estimates and a model for prediction in rapid event-related studies. *NeuroImage*, 25(1), 206–218. <https://doi.org/10.1016/j.neuroimage.2004.11.008>
- Wang, J., Lu, M., Fan, Y., Wen, X., Zhang, R., Wang, B., Ma, Q., Song, Z., He, Y., Wang, J., & Huang, R. (2015). Exploring brain functional plasticity in world class gymnasts: A network analysis. *Brain Structure and Function*, 221, 3503–3519. <https://doi.org/10.1007/s00429-015-1116-6>
- Williams, J., & Krane, V. (2020). *Applied sport psychology: Personal growth to peak performance*. McGraw-Hill Education.
- Wu, G. R., Liao, W., Stramaglia, S., Ding, J. R., Chen, H. F., & Marinazzo, D. (2013). A blind deconvolution approach to recover effective connectivity brain networks from resting state fMRI data. *Medical Image Analysis*, 17(3), 365–374. <https://doi.org/10.1016/j.media.2013.01.003>
- Wu, G. R., & Marinazzo, D. (2015). Retrieving the hemodynamic response function in resting state fMRI: Methodology and applications. *PeerJ PrePrints*, 3, 6050–6053. <https://doi.org/10.7287/peerj.preprints.1317v1>
- Zang, Z., Yan, C., Dong, Z., Huang, J., & Zang, Y. (2012). Granger causality analysis implementation on MATLAB: A graphic user interface toolkit for fMRI data processing. *Journal of Neuroscience Methods*, 203(2), 418–426. <https://doi.org/10.1016/j.jneumeth.2011.10.006>
- Zhang, L. L., Pi, Y. L., Shen, C., Zhu, H., Li, X. P., Ni, Z., Zhang, J., & Wu, Y. (2018). Expertise-level-dependent functionally plastic changes during motor imagery in basketball players. *Neuroscience*, 380, 78–89. <https://doi.org/10.1016/j.neuroscience.2018.03.050>

How to cite this article: Gao, Q., Luo, N., Sun, M., Zhou, W., Li, Y., Liang, M., Yang, C., Zhang, M., Li, R., Gong, L., Yu, J., Leng, J., & Chen, H. (2023). Neural efficiency and proficiency adaptation of effective connectivity corresponding to early and advanced skill levels in athletes of racket sports. *Human Brain Mapping*, 44(2), 388–402. <https://doi.org/10.1002/hbm.26057>